

Coleorhiza-enforced seed dormancy: a novel mechanism to control germination in grasses

Thomas Holloway^{1,2} , Tina Steinbrecher¹ , Marta Pérez¹ , Anne Seville² , David Stock^{2†}, Kazumi Nakabayashi¹  and Gerhard Leubner-Metzger^{1,3} 

¹Department of Biological Sciences, Royal Holloway University of London, Egham, TW20 0EX, UK; ²Syngenta, Jealott's Hill International Research Centre, Warfield, Bracknell, RG42 6EY, UK; ³Laboratory of Growth Regulators, Palacký University and Institute of Experimental Botany, Czech Academy of Sciences, Olomouc CZ-78371, Czech Republic

Summary

Authors for correspondence:

Gerhard Leubner-Metzger

Email: gerhard.leubner@rhul.ac.uk

Kazumi Nakabayashi

Email: kazumi.nakabayashi@rhul.ac.uk

Received: 31 August 2020

Accepted: 4 September 2020

New Phytologist (2020) 0: 2179–2191

doi: 10.1111/nph.16948

Key words: *Avena fatua* (common wild oat), cell wall remodelling enzymes, grass seed dormancy, plant tissue interactions, seed tissue biomechanics, weed management.

- How the biophysical properties of overlaying tissues control growth, such as the embryonic root (radicle) during seed germination, is a fundamental question. In eudicot seeds the endosperm surrounding the radicle confers coat dormancy and controls germination responses through modulation of its cell wall mechanical properties. Far less is known for grass caryopses that differ in tissue morphology. Here we report that the coleorhiza, a sheath-like organ that surrounds the radicle in grass embryos, performs the same role in the grass weed *Avena fatua* (common wild oat).
- We combined innovative biomechanical techniques, tissue ablation, microscopy, tissue-specific gene and enzyme activity expression with the analysis of hormones and oligosaccharides.
- The combined experimental work demonstrates that in grass caryopses the coleorhiza indeed controls germination for which we provide direct biomechanical evidence. We show that the coleorhiza becomes reinforced during dormancy maintenance and weakened during germination. Xyloglucan endotransglycosylases/hydrolases may have a role in coleorhiza reinforcement through cell wall remodelling to confer coat dormancy.
- The control of germination by coleorhiza-enforced dormancy in grasses is an example of the convergent evolution of mechanical restraint by overlaying tissues.

Introduction

The control of developmental phase transitions in plants requires the integration of endogenous and environmental cues. 'Knowing when to grow' depends on plant tissue interactions with hormonal signals and biochemical cell wall remodelling to weaken or stiffen mechanical tissues (Schopfer, 2006; Moulia, 2013; Cosgrove, 2016). Examples in which the growth of root or shoot primordia depend on the mechanical properties of the overlaying tissues are lateral root formation (Lucas *et al.*, 2013; Ramakrishna *et al.*, 2019), bud sprouting (Horvath *et al.*, 2003; Lee *et al.*, 2017), and seed germination (Finch-Savage & Leubner-Metzger, 2006; Nonogaki, 2006; Nambara *et al.*, 2010; Steinbrecher & Leubner-Metzger, 2017, 2018). From a biomechanical perspective a seed consists of two main functional compartments: the embryo that develops a growth potential to expand in response to environmental cues and the tissue layers ('coats') that restrain the growth of the embryo up to a threshold, above which radicle (embryonic root) emergence will occur (Steinbrecher & Leubner-Metzger, 2017). Coat dormancy

imposed by the endosperm tissue is a major dormancy mechanism in many eudicot seeds. In these cases, the micropylar endosperm surrounding the radicle is restraining the growth of the embryo.

Micropylar endosperm weakening is a prerequisite for the completion of seed germination by radicle emergence of Brassicaceae (Müller *et al.*, 2006; Bethke *et al.*, 2007; Linkies *et al.*, 2009; Müller *et al.*, 2009; Graeber *et al.*, 2014), Solanaceae (Chen & Bradford, 2000; Toorop *et al.*, 2000; Chen *et al.*, 2002; Lee *et al.*, 2012; Martinez-Andujar *et al.*, 2012) and other eudicot (Finch-Savage & Leubner-Metzger, 2006; Zhang *et al.*, 2014; Steinbrecher & Leubner-Metzger, 2017) species. This micropylar endosperm weakening is directed by environmentally mediated hormonal mechanisms involving gibberellins (GAs) and ethylene through the activity of cell wall remodelling proteins (CWRPs) such as expansins, glucanases, cellulases, mannanases and transglycosylases that loosen cell wall polysaccharide bonds (Chen & Bradford, 2000; Toorop *et al.*, 2000; Chen *et al.*, 2002; Finch-Savage & Leubner-Metzger, 2006; Linkies *et al.*, 2009; Lee *et al.*, 2012; Martinez-Andujar *et al.*, 2012; Graeber *et al.*, 2014). Abscisic acid (ABA) inhibits seed germination by inhibiting micropylar endosperm weakening and embryo growth (Toorop *et al.*, 2000; Finch-Savage & Leubner-Metzger, 2006; Müller

†This paper is dedicated to the memory of our colleague and friend David Stock.

et al., 2006; Linkies *et al.*, 2009; Martinez-Andujar *et al.*, 2012; Graeber *et al.*, 2014). In dormant Brassicaceae seeds the endosperm is a major site for ABA biosynthesis and release to inhibit germination (Nambara *et al.*, 2010; Kang *et al.*, 2015). Puncture force analysis has been used as a biomechanical technique to reveal the temperature- and hormone-mediated regulation of micropylar endosperm weakening in eudicot seeds (Steinbrecher & Leubner-Metzger, 2017). The endosperm has been proposed to be a mediator of communication in environmental sensing and responses in eudicot seeds (Yan *et al.*, 2014). Weeds have evolved in agricultural systems, where dormancy acts to synchronise their emergence with the cropping cycle to optimise competition with the crop and evade weed management practices (Neve *et al.*, 2009; Sperber *et al.*, 2017; Mohammed *et al.*, 2019).

The diaspores (seed-containing dispersal units) of cereals (barley, wheat, oat), grass weeds (e.g. common wild oat) and other grasses (Poaceae) differ considerably from eudicot seeds (Morrison & Dushnicky, 1982; Sreenivasulu & Wobus, 2013; Rodriguez *et al.*, 2015). They are or contain caryopses, simple dry fruits in which the pericarp (fruit coat) and seed coat are fused, and which are in many cases additionally covered by husks (Fig. 1). In a typical grass caryopsis, the embryonic shoot is contained by the coleoptile (shoot sheath) and the radicle by the coleorhiza (root sheath). Grass embryos lack the micropylar endosperm that plays an important role in eudicot seed dormancy and germination. Instead, the coleorhiza, a nonvascularised embryonic organ that expands upon imbibition, emerges from the caryopsis and is thought to have some role in protecting the growing embryo (Tillich, 2007; Robbertse *et al.*, 2011).

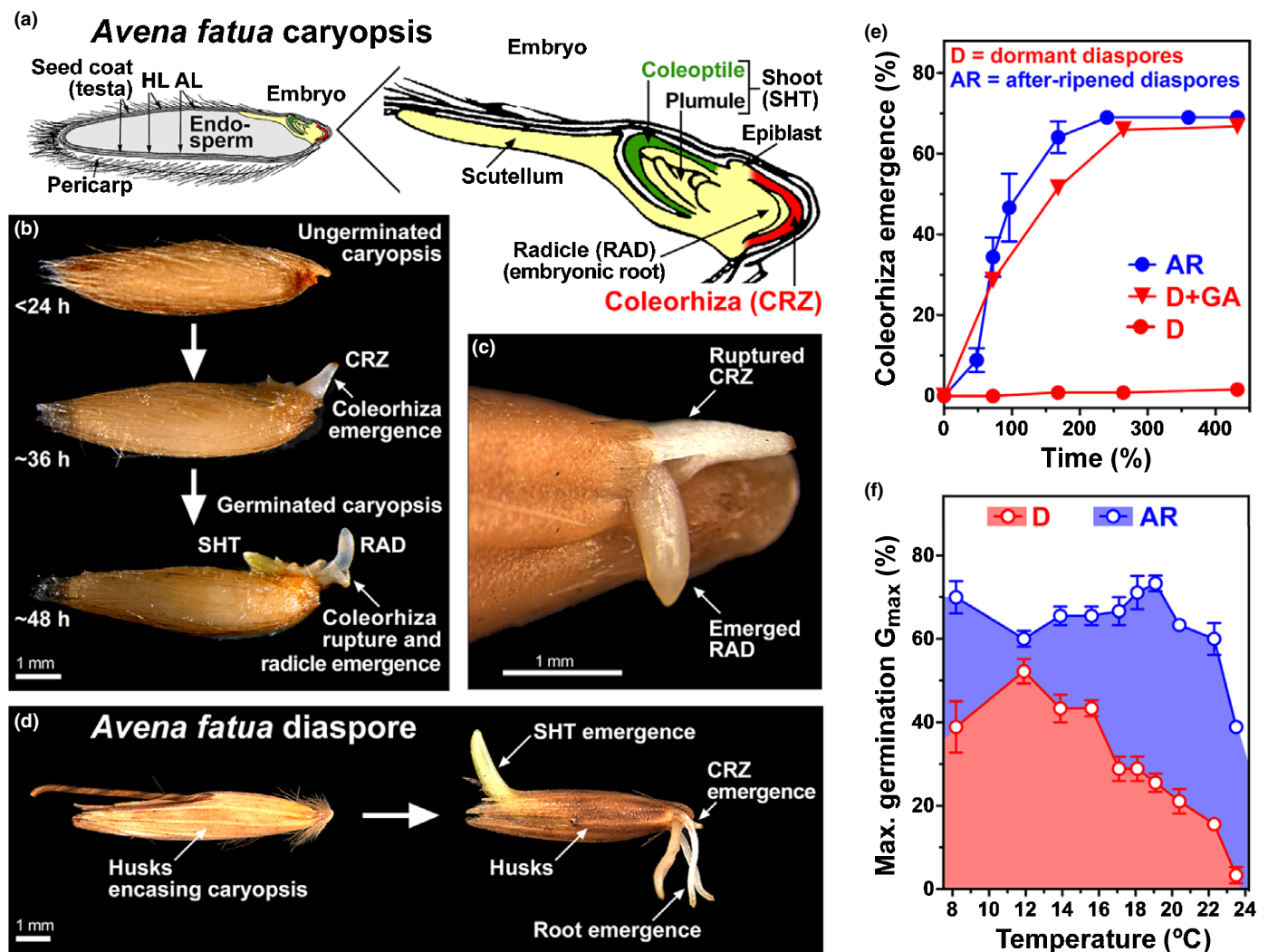


Fig. 1 Morphophysiology of *Avena fatua* germination. (a) Diagrammatic representation of an *A. fatua* caryopsis cut longitudinally (left) and enlarged embryo (right); hyaline layer (HL), aleurone layer (AL), modified from Morrison & Dushnicky (1982), reproduced with permission. (b) Photographs of caryopses at different stages of the germination process, showing the coleorhiza (CRZ) emergence, CRZ rupture by the radicle (RAD) and RAD emergence, and shoot (SHT) emergence. (c) Photograph of CRZ rupture by the emerging RAD of an AR diaspore. (d) Photographs of *A. fatua* diaspore (caryopsis encased by husks) germination, showing CRZ, SHT and root emergence. (e) CRZ emergence of after-ripened (AR) vs dormant (D) diaspores at 20°C; GA, treatment with 50 μ M GA_{4+7} . (f) Effect of different temperatures on the maximum germination (RAD emergence) of D and AR diaspores. Mean values \pm SE for three independent replicates each of 30 individuals.

While the coleorhiza is widespread beyond the grasses in other monocot species and in cycads, it is absent in eudicots. It has been shown in barley that the ABA content of the coleorhiza plays a major role in controlling grass caryopsis dormancy and germination (Millar *et al.*, 2006; Barrero *et al.*, 2009). The authors of these works proposed that the coleorhiza (CRZ) in grasses acts as a barrier to root emergence and is therefore functionally equivalent to the micropylar endosperm in eudicot seeds.

In this study we use the agricultural weed *Avena fatua* L. (common wild oat, Poaceae) to demonstrate that the coleorhiza and the micropylar endosperm are indeed functionally equivalent, in so far as the coleorhiza modulates its mechanical properties to restrain or permit the growth of the radicle during dormancy and germination. We also provide an explanation for how this process may be mediated by xyloglucan endotransglycosylase (XET) enzyme activity localised to the coleorhiza.

Materials and Methods

Seed material and germination assays

Avena fatua L. diaspores were collected in August 2017 from a wheat field in Hampshire, UK. Half of this population was air dried and stored at -20°C ('D' population) and the other half was stored at 50% relative humidity (above a saturated solution of $\text{Ca}(\text{NO}_3)_2$) at 20°C (Supporting Information Fig. S1a). Periodically subpopulations were removed from the humid condition and a germination assay conducted under standard conditions: in a 90 mm Petri-dish containing two filter papers and 5 ml of autoclaved ultrapure water with 30 diaspores in triplicate. All germination experiments were carried out at 20°C under constant light (white fluorescent light at $100\ \mu\text{mol m}^{-2}\ \text{s}^{-1}$, measured with a LI-250 Light Meter; Li-Cor, Bad Homburg, Germany) in a Panasonic MLR-352 Environmental Test Chamber (ETC; Panasonic, Bracknell, UK). This was repeated monthly until no further increase in maximum germination was recorded (112 d) to generate a fully after-ripened (AR) population (Fig. S1a). In order to determine the optimal temperature condition for germination assays (Fig. 1f), dormant (D) and AR diaspores were imbibed on a purpose-built thermogradient plate with a temperature range between 8 and 23°C under constant white light (white bulb light at $16\ \mu\text{mol m}^{-2}\ \text{s}^{-1}$). Here, 20°C was subsequently chosen for the experiments in the ETC because this condition gave the greatest difference in germination between D and AR diaspores with minimal evaporation of water.

Exogenous application of phytohormones and oligosaccharides

For experiments involving ABA application, $50\ \mu\text{M}$ *cis*-S(+)-abscisic acid (Duchefa Biochemie, Haarlem, the Netherlands) was prepared in 1 N KOH and adjusted to pH 7 using HCl. For experiments involving gibberellin (GA) application, $100\ \mu\text{M}$ of a mixture of gibberellin A₄ and A₇ (GA₄₊₇, Duchefa Biochemie, Haarlem, the Netherlands), containing 0.1% (v/v) DMSO was prepared to a neutral pH using KOH. The xyloglucan

heptasaccharide XXXG (Megazyme, Leinster, Ireland) was prepared in ultrapure water to a concentration of 0.1% (w/v) and filter sterilised. The xyloglucan oligosaccharide (Fry *et al.*, 1993) mixture with XXXG, XXLG and XLLG (Megazyme) was used in the same way.

Flow cytometry

Twenty AR caryopses were imbibed at 20°C under constant light for 3, 24 or 48 h and dissected into coleorhiza and plumule tissues on ice. Nuclei were extracted in 100 μl of cystain UV precise P extraction buffer (Sysmec Partec GmbH, Görlitz, Germany) by maceration with a razor blade. Samples were stained with 1 ml of CyStain UV Precise P DAPI fluorescent buffer (Sysmec Partec GmbH) and filtered through a 30- μm filter. Here, >9000 nuclei were analysed using a Partec PAS Flow Cytometer (Sysmec Partec GmbH). Data analysis and noise reduction was performed using FLOWING Software 2.5.1 (Perttu Terho; <http://flowingsoftware.btk.fi>).

Ablation experiments

For experiments involving the ablation of the coleorhiza, a fine grade silica-based sandpaper was used to remove the coleorhiza from dry caryopses (Fig. S4, to be described later). For the ablation of the plumule, a fine razor blade was used to bisect the embryo to the depth of the scutellum and the embryonic shoot (plumule plus coleoptile) removed with fine forceps. In pericarp ablation experiments, the pericarp (plus adhering testa) was peeled away from the embryo using fine forceps without disturbing the underlying tissues. After 240 h, pericarp and plumule ablated treatments were transferred to a plate containing $100\ \mu\text{M}$ GA₄₊₇ to test for germinability.

Microscopy

Partially dissected embryos that had been imbibed for 24 or 48 h under standard conditions were fixed in 4% (w/v) paraformaldehyde and subjected to an ethanol dehydration gradient. The samples were embedded in 2-hydroxyethyl methyl acrylate polymerised with 1% (v/v) benzoyl peroxide (Technovit 7100 cold curing resin system; Kulzer Technique, Wehrheim, Germany) (Yeung & Chan, 2015) following the manufacturer's recommendations but with modifications (Matsushima *et al.*, 2014). Sections of 5 μm thickness were cut on a rotary microtome (HM 355S; Thermo Fisher Scientific, Waltham, MA, USA) and progressively stained with 1% (w/v) safranin O (to stain cell wall lignin) and counterstained with 1% (w/v) toluidine blue (to stain nuclei and polysaccharides) (Ruzin, 1999). Bright-field images were taken using a Nikon Eclipse Ni-E stereomicroscope (Nikon, Tokyo, Japan) and entire images were sharpened and adjusted for brightness, contrast, and tonal range using PHOTOSHOP software (CS6; Adobe, San Jose, CA, USA). Macroscopic images of germination stages were taken using a stereomicroscope (Leica MZ125; Leica Biosystems, Wetzlar, Germany) and images were processed using the inbuilt Leica APPLICATION SUITE Software (v.4.1).

Puncture force measurements

Puncture force was measured directly for isolated coleorhizas using a purpose-built device (Graeber *et al.*, 2014; Steinbrecher & Leubner-Metzger, 2017). Custom-made metal holders held the coleorhizas in place, while a metal probe (0.2 mm diameter) was driven into it at a rate of 0.7 mm min⁻¹, while the resultant forces were measured by a load cell ($F_{\max} = 1$ N). An in-house software platform recorded the resultant force-displacement data and logged puncture force for each sample based on the maximum force sustained by the sample until its rupture. Statistical differences between treatments was inferred using a 2-way ANOVA and between-treatment comparisons were made using Tukey's multiple comparisons test implemented in Graphpad PRISM (v.7.05; GraphPad Software, San Diego, CA, USA).

XET activity assay

Preparations of 50 coleorhizas or radicles were dissected from D or AR caryopses, weighed and frozen in liquid nitrogen. Total protein was extracted from isolated tissues by micropestle homogenisation in 5× (sample w/v) of an extraction buffer containing 200 mM succinate (Na⁺) (pH 5.5) and 2.5 mg ml⁻¹ bovine serum albumin (Fry, 1997) and protein was quantified using the Bradford method (Bradford, 1976). Total protein concentrations were adjusted to 20 µg using the extraction buffer. In total, 5 µl of sample was applied to 6 mm diameter discs of a matrix (EDIPOS, Edenborough, UK) composed of Whatman No. 1 filter paper impregnated with tamarind seed xyloglucan (2.5 g m⁻²) and a sulforhodamine conjugate of the xyloglucan oligosaccharide XLLG (1 µmol m⁻²), held within a 96 well microtitre plate. This plate was incubated at 20°C in the dark for 3 h in container at saturated relative humidity to prevent evaporation. After incubation, the discs were washed repeatedly with ethanol:formic acid:water (1:1:1) followed by water to remove unbound labelled substrate (Fry, 1997) and dried in an oven at 60°C. Fluorescence was measured in a multimode plate reader (SPARK; Tecan Trading AG, Männedorf, Switzerland) by using an excitation filter at 570 nm and emission filter at 615 nm as a mean of 24 independent readings per well in triplicates. Readings were taken before and after sample application, the fraction of substrate bound per well was calculated and blank measurements were subtracted. Based on the known amount of substrate on the membrane, XET activity was calculated as nmol of XLLG transglycosylated. For the XET activity assay involving a gradient of pHs, the same protocol was followed except for the sample preparation, for which individual replicates of 30 isolated embryos were prepared in extraction buffer with pHs adjusted with 10 M NaOH. After extraction, the pH was checked using universal indicators strips.

Separation of XET isozymes by isoelectric focusing (IEF)

Dormant (D) or AR caryopses were imbibed for 48 h under standard conditions. For D caryopses 300 caryopses were dissected into coleorhiza and radicles and, for AR caryopses (or those

treated with ABA), 150 caryopses were dissected on ice. These samples were homogenised using a micropestle in 350 mM succinate (Na⁺) at pH 5.5 on ice and centrifuged at 16 200 *g* to remove cell debris. The supernatant was filtered through a 0.22-µm cellulose acetate spin column (Agilent Technologies, Santa Clara, CA, USA) and desalted against distilled water using a Bio-Rad Bio-Spin 6 column (Bio-Rad Laboratories, Hercules, CA, USA). Total protein concentration was measured (Bradford, 1976). Samples were loaded onto dehydrated IEF strips (Immobiline DryStrip pH 6–11, 13 cm; GE Healthcare, Chicago, IL, USA) according to their relative XET activity as measured at 48 h from the XET activity assay. Equal total XET enzyme activity was loaded for each sample and corresponded to the following protein amounts: AR (coleorhiza 225 µg, radicle 120 µg), ABA (coleorhiza 300 µg, radicle 120 µg), D (coleorhiza 720 µg, radicle 520 µg) in a solution containing 5% glycerol and 2% IPG buffer (pH 6–11; GE Healthcare). Samples in rehydrated gel strips were subjected to an IEF program following the manufacturer's recommendations (8000 V, 16 kVh, current limit 50 µA and power 200 mW) in a flatbed IEF apparatus (3100 OFFGEL fractionator; Agilent Technologies). Gel strips were then equilibrated for 10 min in a buffer containing 50 mM succinate (Na⁺, pH 5.5), 10 mM CaCl₂ and 1 mM dithiothreitol (Iannetta & Fry, 1999). Equilibrated gels were transferred to strips of the substrate matrix previously described and sandwiched between Parafilm and two sheets of glass. This sandwich was incubated in the dark for 24 h. After incubation, unbound fluorescent substrate was removed by washing as previously described (Iannetta & Fry, 1999) and visualised using a UV transilluminator with an orange filter. Images were processed using GIMP software (v.2.8.16; www.gimp.org) to improve the contrast.

RNA extraction, cloning and RT-qPCR experiments

In total, 30 embryos were dissected out of D and AR caryopses previously imbibed for 24 and 48 h. Total RNA was extracted using the RNAqueous™ Total RNA Isolation Kit (Invitrogen) according to manufacturer's instructions. RNA concentration and quality were estimated using a NanoDrop spectrophotometer 1000 (Thermo Scientific). Only samples showing 260/280 nm OD ratios of 1.8 and 260/230 nm over 2.30 were used for the analysis. First strand cDNA was synthesised from 1 µg of total RNA using the Superscript III kit (Invitrogen) as described by Graeber *et al.* (2011) in a 20 µl reaction, either with 12.5 µg ml⁻¹ oligo (dT)_{12–18} for cloning of partial cDNA fragments or 0.3 nmol random pentadecamer (custom made, Eurofins) for samples used for RT-qPCR analysis. Candidate gene sequences were selected from publicly available *Avena* transcriptome datasets (Gutierrez-Gonzalez *et al.*, 2013; Ruduś & Kępczyński, 2018) by similarity-based search using the conserved domain of *XTH* genes and exemplar sequences of the probes on the Affymetrix Barley1 GeneChip. Partial *A. fatua* gene sequences for both candidate and reference genes were cloned using primers designed in GENEIOUS (v.8.1.9) (Table S2). Partial cDNA sequences were amplified, verified by Sanger sequencing and analysed with BLASTN and BLASTX searches.

Gene-specific primers were designed on the cloned sequences (Table S2) and transcript expression was analysed by RT-qPCR as described by Graeber *et al.* (2010, 2011). The data were normalised against the two most stable reference genes (*CAC* and *PP2A*), which were selected out of five candidate reference genes tested using GENEORM software (Vandesompele *et al.*, 2002). Four biological replicates were used for each treatment and time point. Relative expression values were normalised against their respective 24 h values and expressed as fold-change using the $2^{-\Delta\Delta C_t}$ method (Livak & Schmittgen, 2001) for each candidate gene (Fig. 4b).

Results

Avena fatua physiological dormancy, after-ripening and germination

The morphology of the mature caryopsis of *A. fatua* (Morrison & Dushnicky, 1982) was similar to that of cereals and other grasses including that within the embryo, the radicle (embryonic root) is covered by a coleorhiza (Fig. 1a–c). Germination of the actual diaspore, in which the caryopsis was in addition covered by husks, was completed by visible root emergence on the proximal, followed by visible shoot emergence on the distal end (Fig. 1d). Fresh mature *A. fatua* diaspores exhibited physiological dormancy, which is controlled by hormones: ABA is involved in maintaining (Jones *et al.*, 2000) while GA and ethylene are involved in releasing this dormancy (Ruduś *et al.*, 2019). Treatment of dormant (D) *A. fatua* diaspores with GA or 4 months of dry storage ('after-ripening') caused dormancy release (Figs 1e,f, S1) and upon imbibition, emergence of the coleorhiza was the first visible step during the germination process (Fig. 1b,e). Coleorhiza emergence was followed by coleorhiza rupture and the completion of germination by visible radicle emergence (Fig. 1b,c). The precise location of the radicle emergence through the

ruptured coleorhiza was adjacent to the coleorhiza tip and not through the tip itself (Fig. 1c), as has also been observed for barley (Barrero *et al.*, 2009). Dormancy in *A. fatua* acts to inhibit germination under warmer temperatures, a mechanism common in winter annuals, and was associated by the absence of coleorhiza emergence (Fig. 1e). AR diaspores however will germinate under warm conditions (Fig. 1f) with coleorhiza emergence and rupture by the emerging radicle as visible hallmarks (Fig. 1).

Fig. 2(a) shows that coleorhiza emergence, radicle emergence (i.e. the completion of germination) and shoot emergence are three successive visible events in AR caryopses of *A. fatua*. The coleorhiza emergence requires coleorhiza expansion growth to rupture the caryopsis outer covering layer (testa and pericarp). The coleorhiza growth was achieved by visible cell expansion of cells and organ expansion mainly in the longitudinal direction including in regions where the coleorhiza rupture will occur (Fig. 3a). The coleorhiza expansion, which occurs before the growth of the radicle that later ruptures the coleorhiza, was evident from the earlier water uptake and the earlier organ expansion of the coleorhiza compared with the radicle in AR caryopses; neither water uptake nor expansion growth was observed in dormant (D) caryopses (Fig. S2). This mechanism of expansion growth in AR caryopses occurred independently of the cell cycle as coleorhiza cells did not undergo DNA replication (Fig. S3). Treatment of AR caryopses with 50 μM *cis*-S(+)-ABA, a phytohormone associated with the acquisition and maintenance of dormancy, had a disproportionate effect on radicle and shoot emergence (Fig. 2b), indicating that different embryonic organs had autonomous regulation of their rate of expansion. This observed retardation of radicle emergence upon ABA treatment also occurs in eudicot species, such as the endosperm weakening model *Lepidium sativum*, as the result of an inhibition of micropylar endosperm weakening (Müller *et al.*, 2006; Linkies *et al.*, 2009; Graeber *et al.*, 2014). This was the first indication that the coleorhiza may have a role in restraining *A. fatua* radicle expansion.

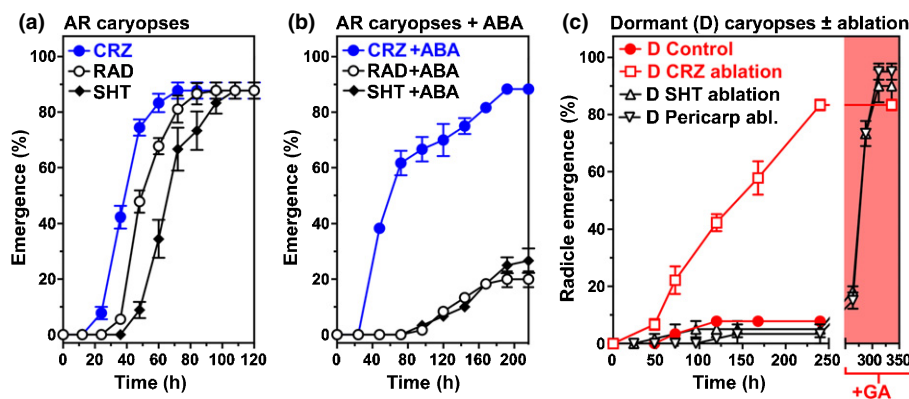


Fig. 2 Germination of after ripened (AR) *Avena fatua* caryopses and ablation experiments with dormant (D) caryopses. (a) Kinetics of coleorhiza (CRZ), radicle (RAD) and shoot (SHT, coleoptile plus plumule) emergence as the three successive visible events during the germination of caryopses in the after-ripened state at 20°C. (b) Effect of 50 μM *cis*-S(+)-abscisic acid (ABA) on the timing of the visible emergence events. (c) Effect of ablation of the CRZ from dormant caryopses in comparison with wounding controls such as the removal of the embryonic shoot and the pericarp (i.e. the embryo overlaying pericarp plus testa). After 240 h, these wounding controls were transferred to a germination promoting medium containing 100 μM GA₄₊₇ to confirm that ablation did not affect to ability to germinate. Mean values \pm SE for three independent replicates each of 30 individuals.

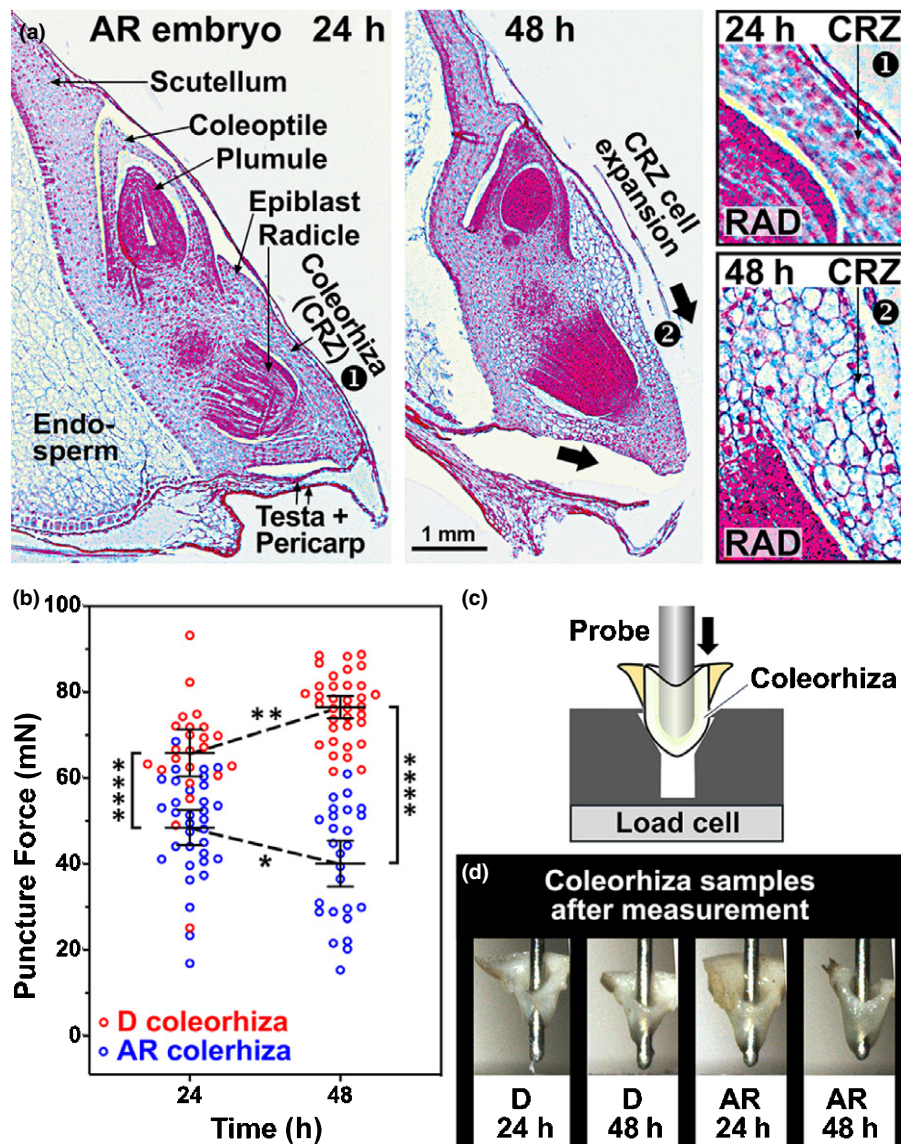


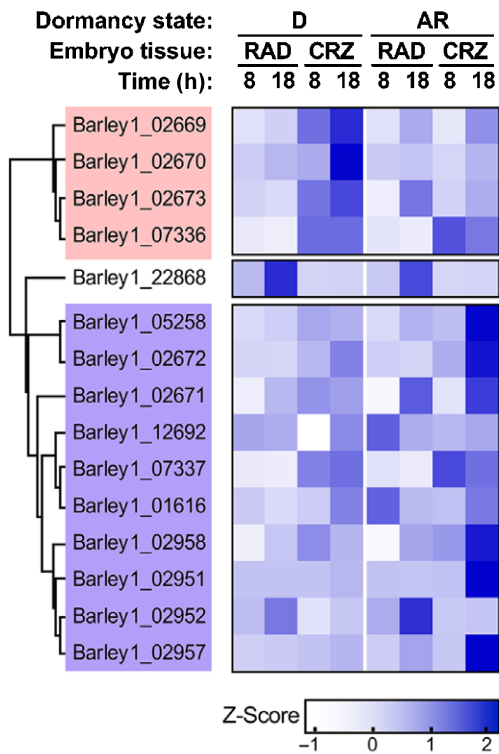
Fig. 3 Microscopy and biomechanical properties of the *Avena fatua* coleorhiza. (a) Bright-field micrographs of the embryo at 24 and 48 h imbibition showing the expansion of the cells of the coleorhiza (CRZ) and the rupture of the covering layers (testa and pericarp); enlarged CRZ (right) correspond to the indicated areas; RAD, radicle. (b) Puncture force measurements for dormant (D) and after-ripened (AR) coleorhizas at 24 and 48 h imbibition where each point represents a single measurement; in addition mean values \pm SE are presented. AR 24 h, $n = 33$; D 24 h, $n = 23$; AR 48 h, $n = 26$; D 48 h, $n = 36$. Significance was inferred using a 2-way ANOVA and between-treatment comparisons were made using Tukey's multiple comparisons test; *, $P < 0.05$; **, $P < 0.01$; ***, $P < 0.001$. For corresponding mechanical stress results see Supporting Information Table S1. (c) Methodology to analyse mechanical properties of the *A. fatua* coleorhizas by puncture force analysis. Graphical representation of the biomechanics approach used to measure coleorhiza puncture force. (d) Example for *A. fatua* coleorhiza samples after the puncture force analysis. The predominant rupture mode in D and AR samples for both time points (24 h, 48 h) was a rupture along one side of the coleorhizas near the tip; that is at the same location as coleorhiza rupture and radicle emergence occurs (Fig. 1c).

Ablation of the coleorhiza breaks dormancy

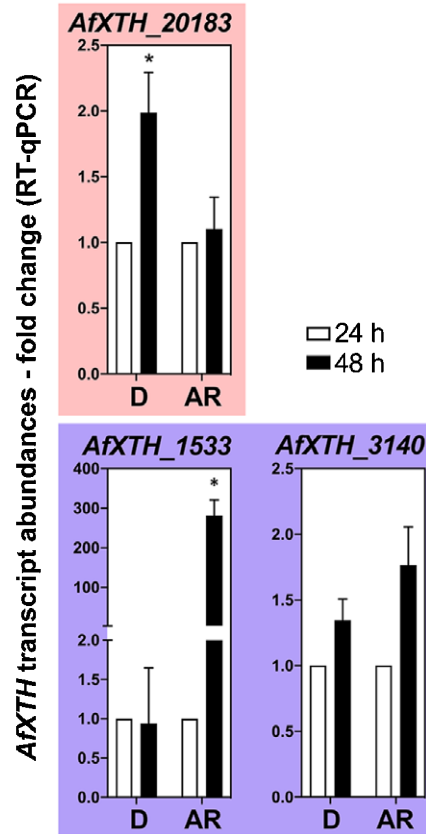
If the coleorhiza restrains the growth of the radicle to maintain dormancy, we hypothesised that coleorhiza ablation from dormant caryopses would induce radicle growth. This was indeed the case as dormant (D) caryopses with the coleorhiza removed by ablation germinated by contrast with the D control (Figs 2c, S4). However, the initiation of radicle growth was delayed and occurred at a slower rate than during germination of AR caryopses, suggesting that physical restraint was not the only factor

controlling radicle expansion growth. We are confident that the dormancy breaking effect of coleorhiza ablation is not a wounding response, as severe wounding treatments, such as the removal of the entire embryonic shoot (SHT), did not induce germination of D caryopses (Fig. 2c). Removal of the testa and pericarp layers covering the embryo (including the coleorhiza) of D caryopses, concurrent with coleorhiza ablation, did not contribute to this effect either, as their ablation had no dormancy breaking effect (Fig. 2c). Caryopsis transfer after these ablation treatments onto plates containing $100 \mu\text{M}$ GA_{4+7} , a strong dormancy

(a) Barley XTH gene expression



(b) *Avena fatua* XTH transcripts



(c) *Avena fatua* XET isozymes

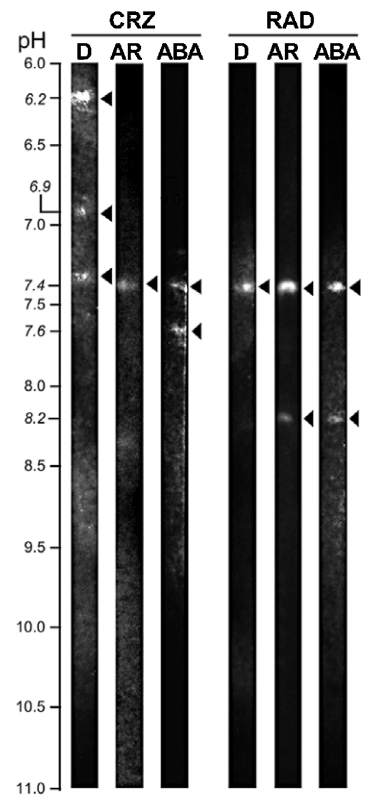


Fig. 4 Tissue-specific and dormancy-specific transcript and isoenzyme expression patterns of XTHs. (a) Heatmap of XTHs identified using a search for the conserved motif ‘DEIDFEFLC’ across Barley1 GeneChip probe sequences. Sequences are arranged according to a tree built from a probe sequence alignment. Mean transcript expression values for dormant (D) and after-ripened (AR) *Hordeum vulgare* coleorhizas and radicles were extracted from publicly available datasets (Barrero *et al.*, 2009) and were normalised by row as z-scores. Note that two major clades of barley XTHs are evident, one upregulated in D (upper panel) and the other in AR (lower panel) coleorhizas. (b) RT-qPCR analysis of transcript expression in *Avena fatua* embryos of *AfXTH_20183* exhibiting the D-clade expression pattern, and *AfXTH_1533* and *AfXTH_3140* exhibiting the AR-clade expression pattern. Mean values \pm SE of four biological replicates are presented. (c) Isoelectric focusing (IEF) zymograms showing the different *Avena fatua* XET isozymes present in D-, AR- and abscisic acid (ABA)-treated radicles and coleorhizas after 48 h of imbibition. White spots show UV fluorescence of a transglycosylated labelled xyloglucan oligosaccharide visualising XET activity at the isoelectric points (pI) of specific XET isozymes (indicated by arrows). In each lane the total protein load was normalised by relative XET activity to represent loading of equal total XET activity. For D tissues, $n = c.$ 300 individuals; for AR tissues $n = c.$ 150 individuals. CRZ, coleorhiza; RAD, radicle.

breaking treatment for *A. fatua* (Fig. S1), demonstrated that the ablation treatments did not have any negative effect on the germinability of the D caryopses (Fig. 2c).

Dormancy state affects the biomechanical properties of the coleorhiza

We hypothesised that, like the micropylar endosperm of many eudicot seeds (Steinbrecher & Leubner-Metzger, 2017), the restraint imposed by the coleorhiza on radicle growth was mechanical in nature. In order to test this hypothesis, we adapted a method previously used to measure the tissue resistance of the micropylar endosperm to quantify the force required by the radicle to rupture the coleorhiza (puncture force, PF) using a custom-made biomechanics platform (Steinbrecher & Leubner-Metzger, 2017). This involved pushing a probe with similar dimensions as the radicle through dormant (D) and AR coleorhizas and measuring the resultant forces

using a load cell (Figs 3b–d, S5). In the AR state, the PF was reduced from 48.4 ± 2.0 to 40.1 ± 2.6 mN between 24 and 48 h of imbibition (Fig. 3b). After 24 h of imbibition, there was a significant difference between D and AR coleorhizas, and after 48 h the PF difference was further increased. In the D state, the PF was increased from 65.8 ± 2.6 to 76.4 ± 1.3 mN between 24 and 48 h (Fig. 3b). That is to say, the AR coleorhiza became weakened over time and the D coleorhiza was strengthened. The difference between PF in the AR state (*c.* 40 mN) and the D state (*c.* 80 mN) are likely to be physiologically relevant, as they are similar to the values measured in models for micropylar endosperm weakening using equivalent methods with the same device; for example *c.* 125 mN (D state) to *c.* 55 mN (AR state) in *L. sativum* (Graeber *et al.*, 2014). We therefore concluded that the coleorhiza is weakened before its rupture in imbibed AR caryopses, but it is strengthened in D caryopses to provide a coleorhiza-enforced dormancy mechanism.

Differential expression of CWRP genes in the coleorhiza

The decrease in puncture force during micropylar endosperm weakening in eudicot seeds is achieved through the activity of CWRPs such as expansins, glucanases, mannanases and xyloglucan endo-transglycosylases/hydrolases (XTHs) (Finch-Savage & Leubner-Metzger, 2006; Steinbrecher & Leubner-Metzger, 2017). CWRP transcripts accumulate in the coleorhiza and radicle of AR *Hordeum vulgare* (glucanases, expansins) and *Brachypodium distachyon* (mannanases) caryopses during germination (Barrero *et al.*, 2009; Gonzalez-Calle *et al.*, 2015). Using microarray (Barley1 GeneChip) expression datasets from Barrero and colleagues (Barrero *et al.*, 2009), we identified additional expansins and cellulases which were upregulated in AR barley coleorhizas (Fig. S6). These CWRPs could therefore be involved in the observed decrease in puncture force (weakening) in AR *A. fatua* coleorhizas (Fig. 3b). We also identified xylosyltransferases which were upregulated in AR barley coleorhizas (Fig. S6), supporting the view that xyloglucan is an important target for complex cell wall loosening and tightening mechanisms (Maris *et al.*, 2009; Lee *et al.*, 2012; Park & Cosgrove, 2015). Interestingly, in their microarray expression experiment with barley caryopses, Barrero and colleagues also identified a probe targeting an XTH (Contig2670_x_at) that was upregulated and highly expressed in dormant (D) coleorhizas compared with AR coleorhizas of barley (Barrero *et al.*, 2009). CWRPs with such an expression pattern could be involved in the observed increase in puncture force (strengthening) of D coleorhizas (Fig. 3b).

Different XTHs have organ- and dormancy-specific transcript and isozyme patterns

The XTH proteins are cell wall remodelling enzymes that modulate cell wall mechanical properties through the remodelling of the hemicellulose xyloglucan (Rose *et al.*, 2002; Frankova & Fry, 2013; Park & Cosgrove, 2015). All tested XTH proteins have xyloglucan endo-transglycosylase enzyme activity (XET, EC 2.4.1.207), but some XTH proteins are known to have in addition xyloglucan endo-hydrolase enzyme activity (XEH, EC 3.2.1.151). We have expanded the analysis of the dormant (D) and AR barley caryopsis microarray datasets (Barrero *et al.*, 2009) by identifying more XTHs by searching for the conserved motif in the active site of XTHs ('DEIDFEFLG'). This search yielded 15 probes that correspond to barley XTHs. Multiple alignment of these probe exemplar sequences identified two clades of XTHs (Fig. 4a). Mapping relative expression data onto this phylogenetic tree showed that these clades have either an expression pattern more associated with barley caryopsis dormancy or germination. For example, one probe (Barley1_02670) was highly expressed specifically in the D coleorhiza, while others (e.g. Barley1_02672) were specifically expressed in the AR coleorhiza. This approach demonstrated that there may be a division of function within the XTH gene family. To identify if similarly distinct XTH transcript expression patterns are evident in *A. fatua* embryos, several candidate *AfXTHs* partial cDNAs were cloned and their expression in whole embryos during imbibition was

quantified using RT-qPCR. The *Avena* contig_20183 (Gutierrez-Gonzalez *et al.*, 2013; Ruduś & Kępczyński, 2018) was similar in sequence to the D-clade XTH from barley (contig_02669, contig_02670, contig_02673; Fig. 4a), whereas *Avena* contig_1533 and contig_3140 were similar in sequence to the AR-clade XTH from barley (contig_02958, contig_01616; Fig. 4a). The transcript abundance of *AfXTH_1533* was found to increase about 300-fold in AR embryos during imbibition, and the one of *AfXTH_3140* may also increase slightly (Fig. 4b). By contrast to these *AfXTHs*, the transcript abundance of *AfXTH_20183* significantly increased in D embryos during imbibition (Fig. 4b). These findings demonstrated that both *A. fatua* and barley have XTH transcripts that are specifically upregulated either in the AR or in D state.

To test the hypothesis that there are dormancy-specific and germination-specific XTHs present in different embryonic organs in *A. fatua*, we used an IEF separation over a pH gradient coupled with a zymographic visualisation based on their XET enzyme activity to reveal their isoelectric points (pI) (Fig. 4c); equal amounts of total XET enzyme activity were loaded in each IEF lane. In the radicle (RAD) we found that, in the D and AR states, and an ABA treatment, XET isozymes are similar, one major isozyme with pI 7.4 and a minor isozyme in the AR and ABA treatments with pI 8.2. The same pattern was evident in the AR coleorhiza (CRZ), however the D coleorhiza had a different pattern of more acidic isozymes (pI 6.2 and pI 6.9). ABA-treated AR coleorhizas had the major isozyme with pI 7.4 as the other AR treatments with an additional isozyme with pI 7.6. These results demonstrated that there were XTHs specific to the D coleorhiza, and that dormancy-related changes in XET isozyme profile were occurring in the coleorhiza and not the radicle.

XET enzyme activities differ between D and AR embryo organs

To further test the hypothesis that the XET isozyme profile in dormant (D) and AR states are functionally different, we quantified the total XET enzyme activities of tissue lysate from whole D and AR embryos of *A. fatua* across a spectrum of pHs (Fig. 5a). For the XET enzyme activity assays we used a fluorescently labelled xyloglucan oligosaccharide (XLLG-SR) as substrate (Fig. S7; Fry, 1997). We hypothesised that XET activity in the germinating AR state would be optimal at lower pHs as apoplastic pH is typically lower in expanding tissues (Arsuffi & Braybrook, 2018). The embryo protein extract's XET enzyme activity pH optimum in the AR state was indeed lower than in the D state (Fig. 5a). The total XET enzyme activity against the substrate used was *c.* three-fold lower in the D compared with the AR embryos.

We then used the XET assay to compare the enzyme activities of coleorhiza and radicle tissues. Abscisic acid application reduced XET activity only in the coleorhiza, but not in the radicle of AR embryos (Fig. 5b). During imbibition, XET enzyme activity accumulated in the coleorhiza and radicle in AR caryopses, but not in D caryopses (Fig. 5c). This XET activity accumulation in AR caryopses was not directly related to the

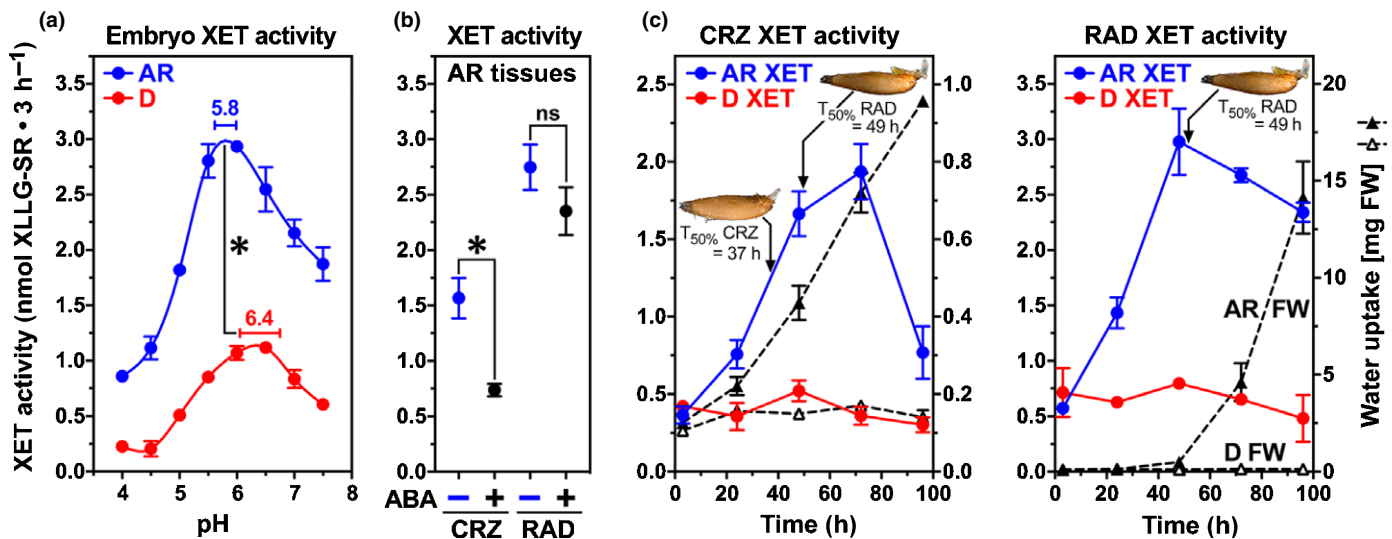


Fig. 5 Dynamics of XET activity from tissue protein extracts. (a) Effect of pH on XET activity in protein extracts of isolated dormant (D) and after-ripened (AR) embryos imbibed for 48 h. Horizontal error bars show the 95% confidence interval for the optimum pH generated through a segmental linear regression model. (b) Effect of ABA (50 μ M) treatment on XET activity in AR coleorhizas and radicles (RAD). Significance was calculated using a one-way ANOVA: *, $P < 0.05$. (c) Dynamics of XET activity over time in D and AR coleorhizas (left panel) and radicles (right panel) plotted against the change in CRZ and RAD fresh weight (FW) due to water uptake. The time taken for the AR populations to reach 50% cumulative coleorhiza and radicle emergence ($T_{50\%}$ CRZ, $T_{50\%}$ RAD) are indicated and shown by arrows. Mean values \pm SE for triplicates of c. 50 individuals are presented.

expansion of tissues as measured by water uptake, as after 72 h in the coleorhiza and 48 h in the radicle XET activity levels declined even though expansion of the tissues continued (Figs 3, 5c). The peak of XET activity in the coleorhiza was closer in timing to the emergence of the radicle than the expansion of the coleorhiza, indicating that XET activity may play more of a role in the weakening of the coleorhiza observed from the puncture force measurements rather than in the expansion of the coleorhiza itself. Certain XET isozymes therefore seemed to correlate with coleorhiza weakening and rupture during the germination of AR caryopses (Figs 3, 4).

Xyloglucan oligosaccharides modify germination behaviour

In the absence of XTH mutants in monocots or specific XET enzyme inhibitors (Chormova *et al.*, 2015) we aimed to test if XTHs were also implicated in coleorhiza tissue reinforcement as suggested from division of function within the XTH gene family in barley (Fig. 4a), Contig2670_x_at transcripts accumulating in D barley coleorhiza (Barrero *et al.*, 2009) and distinct XTH transcripts (Fig. 4b, *AfXTH_20183*) and XET isozymes in dormant (D) were compared with AR *A. fatua* coleorhiza (Fig. 4b). To investigate this, we applied an excess of xyloglucan oligosaccharide (XXXG; Fig. S8a) to AR *A. fatua* caryopses and analysed if this changed their germination behaviour (Fig. 6). While application of XXXG to AR caryopses did not affect coleorhiza emergence, it slightly delayed germination (radicle emergence). It however did not appreciably affect the maximal germination percentage of the population (Fig. 6a). The observed germination delay was small compared with ABA application, which also delayed germination without appreciably affecting maximal germination. Seedling size was not visibly affected by the XXXG treatment, but the ABA delayed germination was also associated

with smaller seedlings (Fig. 6b). However, when XXXG was applied in combination with ABA, radicle emergence was completely inhibited (Fig. 6a) and germination was arrested at the coleorhiza emergence stage (Fig. 6b). The same result was obtained with a combination of three xyloglucan oligosaccharides (Fig. S8b). We propose that this germination arrest involving xyloglucans indicated that XTHs play a role in a coleorhiza-enforced dormancy mechanism by strengthening the cell walls of the coleorhiza to inhibit coleorhiza rupture and radicle emergence.

Discussion

Convergent evolution of the coleorhiza and micropylar endosperm to control germination by dormancy

Our measurement of changes in the tissue resistance of the coleorhiza in dormant (D) and AR states of *A. fatua* caryopses (Fig. 3b) directly demonstrated that the dynamic mechanical properties of the coleorhiza, like the micropylar endosperm of mature eudicot seeds, controlled radicle emergence as a coat dormancy mechanism. We therefore provided explicit evidence from direct biomechanical measurement that the coleorhiza indeed acted as a key organ preventing root emergence (germination) of dormant caryopses, a hypothesis that was first proposed based on a comparison of barley coleorhiza ABA metabolism and sensitivities, as well as barley coleorhiza transcriptomes in the D and AR states (Millar *et al.*, 2006; Barrero *et al.*, 2009). Further evidence in support for this coleorhiza-enforced dormancy mechanism comes from microscopic and organ (coleorhiza and radicle) elongation and rupture analyses comparing D and AR caryopses of barley (Barrero *et al.*, 2009) and *A. fatua* (our work). Furthermore, our ablation experiments provided further direct support

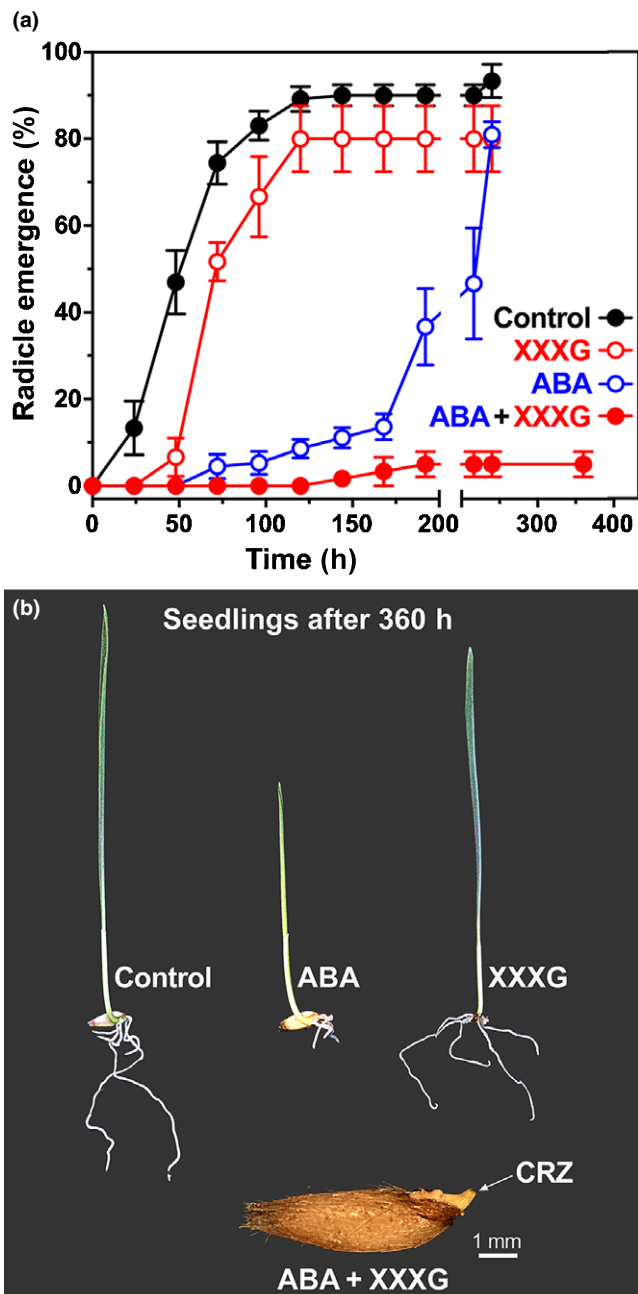


Fig. 6 Effect of the xyloglucan oligosaccharide XXXG on *Avena fatua* germination. (a) Germination curves showing the effects of 50 μ M abscisic acid (ABA), 0.1% (w/v) XXXG and a combination of both on radicle emergence of after-ripened (AR) caryopses. (b) Photographs of the seedling growth symptoms produced by the treatments in the germination assay. A combination of XXXG and ABA causes germination arrest at coleorhiza emergence. Images of individual seedlings are representative of the symptoms seen in the different treatments. Mean values \pm SE for triplicates each of 30 caryopses are presented.

for a key role of the coleorhiza in the coat-enforced dormancy of *A. fatua* (Fig. 2c). Depending on the grass species, different covering structures (including the husks) can confer coat dormancy (Nambara *et al.*, 2010; Rodriguez *et al.*, 2015). The coleorhiza therefore forms part of a whole-seed system of covering layers that controls dormancy and germination. This dormancy is

maintained by ABA and released by GA, and dormancy level is of key importance for preharvest sprouting in cereals. Interestingly, the *MOTHER-OF-FT-AND-TFL1* (*MFT*) dormancy gene is highly expressed in the endosperm of dormant eudicot seeds (Vaistij *et al.*, 2018) as well as in the coleorhiza of D wheat (Nakamura *et al.*, 2011) caryopses, further supporting the hypothesis that the micropylar endosperm and the coleorhiza serve similar roles in conferring diaspore dormancy.

Although the micropylar endosperm and coleorhiza share similar anatomical compartments, as organs surrounding the radicle in both monocot and eudicot diaspores, the micropylar endosperm and coleorhiza have distinct developmental origins. The micropylar endosperm is a triploid endospermic tissue formed from the double fertilisation of polar nuclei (Sreenivasulu & Wobus, 2013; Yan *et al.*, 2014), whereas the coleorhiza is proposed to be homologous to the hypocotyl or suspensor (Tillich, 2007; Robbertse *et al.*, 2011). The coleorhiza is widespread beyond the grasses in other monocot species and in cycads but is absent in eudicots. Upon dormancy release, GA and ethylene induce the expression of CWRP genes including expansins, cellulases, mannanases and XTHs in the micropylar endosperm of eudicot seeds (Chen & Bradford, 2000; Toorop *et al.*, 2000; Chen *et al.*, 2002; Finch-Savage & Leubner-Metzger, 2006; Linkies *et al.*, 2009; Lee *et al.*, 2012; Martinez-Andujar *et al.*, 2012; Graeber *et al.*, 2014) and the coleorhiza of Poaceae caryopses (Millar *et al.*, 2006; Barrero *et al.*, 2009; Gonzalez-Calle *et al.*, 2015; Ruduś *et al.*, 2019) including *A. fatua* (this work). Interestingly, expansins are also expressed in the overlaying tissues during lateral root formation and the importance of the mechanical properties and of tissue interactions was proposed (Lucas *et al.*, 2013; Ramakrishna *et al.*, 2019). The convergent evolution of mechanical restraint of overlaying tissues lends support to the concept that mechanical interactions are important determinants promoting root (radicles during germination as well as lateral roots) emergence. In agreement with this, the lack of mechanical restraint weakening (Graeber *et al.*, 2014; Steinbrecher & Leubner-Metzger, 2017) or active mechanical restraint strengthening (Fig. 3b) provided a suitable dormancy mechanism as it blocks the completion of germination by radicle emergence.

XTHs as candidate reinforcement genes to confer coleorhiza-enforced seed dormancy

While only weakening or the lack of mechanical restraint weakening has been reported in the micropylar endosperm of eudicot seeds (Graeber *et al.*, 2014; Steinbrecher & Leubner-Metzger, 2017), we reported here that the coleorhiza becomes reinforced during the maintenance of dormancy of *A. fatua* (Fig. 3b). We propose that this reinforcement is the result of active coleorhiza cell wall strengthening processes that include xyloglucan remodelling as a target. Many species have a large number of XTH genes (e.g. 33 in *Arabidopsis thaliana*) (Rose *et al.*, 2002). GUS reporter lines have demonstrated that individual XTHs have highly tissue-specific expression patterns (Becnel *et al.*, 2006) that are likely to play a role in pH, temperature and substrate specificity (Hrmova *et al.*, 2009; Maris *et al.*, 2009, 2010). Across the

conditions tested, we identified two acidic XET isozymes (pI 6.2 and pI 6.9) that are unique to the dormant coleorhiza; these are neither present in the AR state coleorhiza, nor in the radicle at any state. Similarly, in *A. thaliana*, a seed-specific XTH (*XTH25*, At5g57550) is specifically expressed only in the micropylar endosperm of D seeds of the Cape Verde Islands (CVI) ecotype (Dekkers *et al.*, 2016). The physiological result of XET activity is substrate-dependant, with loosening and reinforcement effects observed depending on exogenous application of different xyloglucan oligosaccharides (Vissenberg *et al.*, 2000; Takeda *et al.*, 2002; Hrmova *et al.*, 2009). It is known from these works that extraprotoplasmatic XETs incorporate the xyloglucan oligosaccharides into the cell wall, leading to either loosening or reinforcement of the cellulose-xyloglucan network. We found that exogenous application of XXXG (a xyloglucan heptasaccharide) slightly delayed coleorhiza rupture and radicle emergence in AR caryopses however, when applied together with ABA, germination is arrested at the coleorhiza emergence step. While our results did not provide direct evidence for a role of XTHs in coleorhiza cell wall reinforcement or weakening, the presence of ABA inducible and dormancy-specific XET isozymes in the coleorhiza and the observation that xyloglucan oligosaccharide application can arrest germination at the coleorhiza emergence step lent support to the working hypothesis that XTHs are involved in coleorhiza reinforcement by strengthening the cell wall. To provide direct evidence for this requires determining the precise cell wall remodelling mechanisms involved in the process of coleorhiza-enforced dormancy. An understanding of the convergent function of the micropylar endosperm and coleorhiza will contribute to an improved understanding of key agronomic issues such as preharvest sprouting (Nambara *et al.*, 2010; Rodriguez *et al.*, 2015), germplasm quality, seedling vigour and grass weed management. Our biomechanical and ablation experiments provided direct evidence for coleorhiza-enforced seed dormancy as a novel mechanism to control germination in grasses.







Acknowledgements

We thank Mark Levy, Diane Grant and Sarah Rabjohn for assistance with seed processing and Paul Fraser and Chris Gerrish for materials and technical assistance with IEF. This work was supported by Biotechnology and Biological Sciences Research Council (BBSRC) Research Grants (BB/M02203X/1, BB/R505730/1) to GL-M. The development of methods for analysing coleorhiza biomechanics was supported by the a BBSRC Research Grant (BB/M000583/1) to TS and GL-M. The authors declare no competing interests.

Author contributions

TH, TS, KN, DS, AS and GL-M planned and designed the research; TH, MP and TS performed experiments; AS provided access to materials; TH, MP, TS, KN and GL-M analysed and interpreted the data; TH, KN and GL-M wrote the manuscript with contributions from all authors.

ORCID

Thomas Holloway  <https://orcid.org/0000-0002-8753-7841>
Gerhard Leubner-Metzger  <https://orcid.org/0000-0002-6045-8713>
Kazumi Nakabayashi  <https://orcid.org/0000-0002-4186-541X>
Marta Pérez  <https://orcid.org/0000-0002-6802-205X>
Anne Seville  <https://orcid.org/0000-0001-8024-7959>
Tina Steinbrecher  <https://orcid.org/0000-0003-3282-6029>

Data availability

All data presented or analysed in this published article are available online through figshare <https://doi.org/10.6084/m9.figshare.12894020>.

References

- Arsuffi G, Braybrook SA. 2018. Acid growth: an ongoing trip. *Journal of Experimental Botany* 69: 137–146.
- Barrero JM, Talbot MJ, White RG, Jacobsen JV, Gubler F. 2009. Anatomical and transcriptomic studies of the coleorhiza reveal the importance of this tissue in regulating dormancy in barley. *Plant Physiology* 150: 1006–1021.
- Becnal J, Natarajan M, Kipp A, Braam J. 2006. Developmental expression patterns of *Arabidopsis* XTH genes reported by transgenes and geneinvestigator. *Plant Molecular Biology* 61: 451–467.
- Bethke PC, Libourel IGL, Aoyama N, Chung Y-Y, Still DW, Jones RL. 2007. The *Arabidopsis* aleurone layer responds to nitric oxide, gibberellin, and abscisic acid and is sufficient and necessary for seed dormancy. *Plant Physiology* 143: 1173–1188.
- Bradford MM. 1976. A rapid and sensitive method for the quantification of microgram quantities of protein utilizing the principle of protein-dye binding. *Analytical Biochemistry* 72: 248–254.
- Chen F, Bradford KJ. 2000. Expression of an expansin is associated with endosperm weakening during tomato seed germination. *Plant Physiology* 124: 1265–1274.
- Chen F, Nonogaki H, Bradford KJ. 2002. A gibberellin-regulated xyloglucan endotransglycosylase gene is expressed in the endosperm cap during tomato seed germination. *Journal of Experimental Botany* 53: 215–223.
- Chormova D, Frankova L, Defries A, Cutler SR, Fry SC. 2015. Discovery of small molecule inhibitors of xyloglucan endotransglucosylase (XET) activity by high-throughput screening. *Phytochemistry* 117: 220–236.
- Cosgrove DJ. 2016. Plant cell wall extensibility: connecting plant cell growth with cell wall structure, mechanics, and the action of wall-modifying enzymes. *Journal of Experimental Botany* 67: 463–476.
- Dekkers BJ, Pearce SP, van Bolderen-Veldkamp RP, Holdsworth MJ, Bentsink L. 2016. Dormant and after-ripened *Arabidopsis thaliana* seeds are distinguished by early transcriptional differences in the imbibed state. *Frontiers in Plant Science* 7: 1323.
- Finch-Savage WE, Leubner-Metzger G. 2006. Seed dormancy and the control of germination. *New Phytologist* 171: 501–523.
- Frankova L, Fry SC. 2013. Biochemistry and physiological roles of enzymes that cut and paste plant cell-wall polysaccharides. *Journal of Experimental Botany* 64: 3519–3550.
- Fry SC. 1997. Novel 'dot-blot' assays for glycosyltransferases and glycosylhydrolases: optimization for xyloglucan endotransglycosylase (XET) activity. *The Plant Journal* 11: 1141–1150.
- Fry SC, York WS, Albersheim P, Darvill A, Hayashi T, Joseleau JP, Kato Y, Lorences EP, MacLachlan GA, Mcneil M *et al.* 1993. An unambiguous nomenclature for xyloglucan-derived oligosaccharides. *Physiologia Plantarum* 89: 1–3.

- González-Calle V, Barrero-Sicilia C, Carbonero P, Iglesias-Fernández R. 2015. Mannans and endo-beta-mannanases (MAN) in *Brachypodium distachyon*: expression profiling and possible role of the *BdMAN* genes during coleorhiza-limited seed germination. *Journal of Experimental Botany* 66: 3753–3764.
- Graeber K, Linkies A, Müller K, Wunchova A, Rott A, Leubner-Metzger G. 2010. Cross-species approaches to seed dormancy and germination: conservation and biodiversity of ABA-regulated mechanisms and the Brassicaceae DOG1 genes. *Plant Molecular Biology* 73: 67–87.
- Graeber K, Linkies A, Steinbrecher T, Mummenhoff K, Tarkovská D, Turečková V, Ignatz M, Sperber K, Voegele A, de Jong H *et al.* 2014. *DELAY OF GERMINATION 1* mediates a conserved coat dormancy mechanism for the temperature- and gibberellin-dependent control of seed germination. *Proceedings of the National Academy of Sciences, USA* 111: E3571–E3580.
- Graeber K, Linkies A, Wood A, Leubner-Metzger G. 2011. A guideline to family-wide comparative state-of-the-art quantitative RT-PCR analysis exemplified with a Brassicaceae cross-species seed germination case study. *Plant Cell* 23: 2045–2063.
- Gutiérrez-González JJ, Tu ZJ, Garvin DF. 2013. Analysis and annotation of the hexaploid oat seed transcriptome. *BMC Genomics* 14: 471.
- Horvath DP, Anderson JV, Chao WS, Foley ME. 2003. Knowing when to grow: signals regulating bud dormancy. *Trends in Plant Science* 8: 534–540.
- Hrmova M, Farkas V, Harvey AJ, Lahnstein J, Wischmann B, Kaewthai N, Ezcurra I, Teeri TT, Fincher GB. 2009. Substrate specificity and catalytic mechanism of a xyloglucan xyloglucosyl transferase HvXET6 from barley (*Hordeum vulgare* L.). *FEBS Journal* 276: 437–456.
- Iannetta PPM, Fry SC. 1999. Visualization of the activity of xyloglucan endotransglycosylase (XET) isoenzymes after gel electrophoresis. *Phytochemical Analysis* 10: 238–240.
- Jones HD, Kurup S, Peters NCB, Holdsworth MJ. 2000. Identification and analysis of proteins that interact with the *Avena fatua* homologue of the maize transcription factor VIVIPAROUS 1. *The Plant Journal* 21: 133–142.
- Kang J, Yim S, Choi H, Kim A, Lee KP, Lopez-Molina L, Martinoia E, Lee Y. 2015. Abscisic acid transporters cooperate to control seed germination. *Nature Communications* 6: 8113.
- Lee KJD, Dekkers BJW, Steinbrecher T, Walsh CT, Bacic A, Bentsink L, Leubner-Metzger G, Knox JP. 2012. Distinct cell wall architectures in seed endosperms in representatives of the Brassicaceae and Solanaceae. *Plant Physiology* 160: 1551–1566.
- Lee Y, Karunakaran C, Lahlali R, Liu X, Tanino KK, Olsen JE. 2017. Photoperiodic regulation of growth-dormancy cycling through induction of multiple bud-shoot barriers preventing water transport into the winter buds of Norway spruce. *Frontiers in Plant Science* 8: 2109.
- Linkies A, Müller K, Morris K, Turečková V, Cadman CSC, Corbineau F, Strnad M, Lynn JR, Finch-Savage WE, Leubner-Metzger G. 2009. Ethylene interacts with abscisic acid to regulate endosperm rupture during germination: a comparative approach using *Lepidium sativum* and *Arabidopsis thaliana*. *Plant Cell* 21: 3803–3822.
- Livak KJ, Schmittgen TD. 2001. Analysis of relative gene expression data using real-time quantitative PCR and the $2^{-\Delta\Delta CT}$ method. *Methods* 25: 402–408.
- Lucas M, Kenobi K, von Wangenheim D, Vobeta U, Swarup K, De Smet I, Van Damme D, Lawrence T, Peret B, Moscardi E *et al.* 2013. Lateral root morphogenesis is dependent on the mechanical properties of the overlaying tissues. *Proceedings of the National Academy of Sciences, USA* 110: 5229–5234.
- Maris A, Kaewthai N, Eklöf JM, Miller JG, Brumer H, Fry SC, Verbelen JP, Vissenberg K. 2010. Differences in enzymic properties of five recombinant xyloglucan endotransglucosylase/hydrolase (XTH) proteins of *Arabidopsis thaliana*. *Journal of Experimental Botany* 62: 261–271.
- Maris A, Suslov D, Fry SC, Verbelen JP, Vissenberg K. 2009. Enzymic characterization of two recombinant xyloglucan endotransglucosylase/hydrolase (XTH) proteins of *Arabidopsis* and their effect on root growth and cell wall extension. *Journal of Experimental Botany* 60: 3959–3972.
- Martínez-Andujar C, Pluskota WE, Bassel GW, Asahina M, Püpel P, Nguyen TT, Takeda-Kamiya N, Toubiana D, Bai B, Gorecki RJ *et al.* 2012. Mechanisms of hormonal regulation of endosperm cap-specific gene expression in tomato seeds. *The Plant Journal* 71: 575–586.
- Matsushima R, Maekawa M, Kusano M, Kondo H, Fujita N, Kawagoe Y, Sakamoto W. 2014. Amyloplast-localized SUBSTANDARD STARCH GRAIN4 protein influences the size of starch grains in rice endosperm. *Plant Physiology* 164: 623–636.
- Millar AA, Jacobsen JV, Ross JJ, Helliwell CA, Poole AT, Scofield G, Reid JB, Gubler F. 2006. Seed dormancy and ABA metabolism in *Arabidopsis* and barley: the role of ABA 8'-hydroxylase. *The Plant Journal* 45: 942–954.
- Mohammed S, Turckova V, Tarkowska D, Strnad M, Mummenhoff K, Leubner-Metzger G. 2019. Pericarp-mediated chemical dormancy controls the fruit germination of the invasive hoary cress (*Lepidium draba*), but not of hairy whitetop (*Lepidium appelianum*). *Weed Science* 67: 560–571.
- Morrison IN, Dushnicky L. 1982. Structure of the covering layers of the wild oat (*Avena fatua*) caryopsis. *Weed Science* 30: 352–359.
- Mouliat B. 2013. Plant biomechanics and mechanobiology are convergent paths to flourishing interdisciplinary research. *Journal of Experimental Botany* 64: 4617–4633.
- Müller K, Linkies A, Vreeburg RAM, Fry SC, Krieger-Liszczay A, Leubner-Metzger G. 2009. *In vivo* cell wall loosening by hydroxyl radicals during cress (*Lepidium sativum* L.) seed germination and elongation growth. *Plant Physiology* 150: 1855–1865.
- Müller K, Tintelnot S, Leubner-Metzger G. 2006. Endosperm-limited Brassicaceae seed germination: Abscisic acid inhibits embryo-induced endosperm weakening of *Lepidium sativum* (cress) and endosperm rupture of cress and *Arabidopsis thaliana*. *Plant & Cell Physiology* 47: 864–877.
- Nakamura S, Abe F, Kawahigashi H, Nakazono K, Tagiri A, Matsumoto T, Utsugi S, Ogawa T, Handa H, Ishida H *et al.* 2011. A wheat homolog of MOTHER OF FT AND TFL1 acts in the regulation of germination. *Plant Cell* 23: 3215–3229.
- Nambara E, Okamoto M, Tatematsu K, Yano R, Seo M, Kamiya Y. 2010. Abscisic acid and the control of seed dormancy and germination. *Seed Science Research* 20: 55–67.
- Neve P, Vila-Aiub M, Roux F. 2009. Evolutionary-thinking in agricultural weed management. *New Phytologist* 184: 783–793.
- Nonogaki H. 2006. Seed germination – the biochemical and molecular mechanisms. *Breeding Science* 56: 93–105.
- Park YB, Cosgrove DJ. 2015. Xyloglucan and its interactions with other components of the growing cell wall. *Plant & Cell Physiology* 56: 180–194.
- Ramakrishna P, Ruiz Duarte P, Rance GA, Schubert M, Vordermaier V, Vu LD, Murphy E, Vilches Barro A, Swarup K, Moirangthem K *et al.* 2019. EXPANSIN A1-mediated radial swelling of pericycle cells positions anticlinal cell divisions during lateral root initiation. *Proceedings of the National Academy of Sciences, USA* 116: 8597–8602.
- Robertse HPJ, Grobbelaar N, du Toit E. 2011. Origin of the coleorhiza in cycad seedlings and its structural homology with that of the Poaceae. *Botanical Review* 77: 1–10.
- Rodríguez MV, Barrero JM, Corbineau F, Gubler F, Benech-Arnold RL. 2015. Dormancy in cereals (not too much, not so little): about the mechanisms behind this trait. *Seed Science Research* 25: 99–119.
- Rose JK, Braam J, Fry SC, Nishitani K. 2002. The XTH family of enzymes involved in xyloglucan endotransglucosylation and endohydrolysis: current perspectives and a new unifying nomenclature. *Plant & Cell Physiology* 43: 1421–1435.
- Ruduš I, Cembrowska-Lech D, Jaworska A, Kepczyński J. 2019. Involvement of ethylene biosynthesis and perception during germination of dormant *Avena fatua* L. caryopses induced by KAR₁ or GA₃. *Planta* 249: 719–738.
- Ruduš I, Kepczyński J. 2018. Reference gene selection for molecular studies of dormancy in wild oat (*Avena fatua* L.) caryopses by RT-qPCR method. *PLoS ONE* 13: e0192343.
- Ruzin SE. 1999. *Plant microtechnique and microscopy*. Oxford, UK & New York, NY, USA: Oxford University Press.
- Schopfer P. 2006. Biomechanics of plant growth. *American Journal of Botany* 93: 1415–1425.
- Sperber K, Steinbrecher T, Graeber K, Scherer G, Clausing S, Wiegand N, Hourston JE, Kurre R, Leubner-Metzger G, Mummenhoff K. 2017. Fruit fracture biomechanics and the release of *Lepidium didymum* pericarp-imposed mechanical dormancy by fungi. *Nature Communications* 8: 1868.
- Sreenivasulu N, Wobus U. 2013. Seed-development programs: a systems biology-based comparison between dicots and monocots. *Annual Review of Plant Biology* 64: 189–217.

- Steinbrecher T, Leubner-Metzger G. 2017. The biomechanics of seed germination. *Journal of Experimental Botany* **68**: 765–783.
- Steinbrecher T, Leubner-Metzger G. 2018. Tissue and cellular mechanics of seeds. *Current Opinion in Genetics and Development* **51**: 1–10.
- Takeda T, Furuta Y, Awano T, Mizuno K, Mitsuishi Y, Hayashi T. 2002. Suppression and acceleration of cell elongation by integration of xyloglucans in pea stem segments. *Proceedings of the National Academy of Sciences, USA* **99**: 9055–9060.
- Tillich HJ. 2007. Seedling diversity and the homologies of seedling organs in the order Poales (Monocotyledons). *Annals of Botany* **100**: 1413–1429.
- Toorop PE, van Aelst AC, Hilhorst HWM. 2000. The second step of the biphasic endosperm cap weakening that mediates tomato (*Lycopersicon esculentum*) seed germination is under control of ABA. *Journal of Experimental Botany* **51**: 1371–1379.
- Vaistij FE, Barros-Galvao T, Cole AF, Gilday AD, He ZS, Li Y, Harvey D, Larson TR, Graham IA. 2018. MOTHER-OF-FT-AND-TFL1 represses seed germination under far-red light by modulating phytohormone responses in *Arabidopsis thaliana*. *Proceedings of the National Academy of Sciences, USA* **115**: 8442–8447.
- Vandesompele J, De Preter K, Pattyn F, Poppe B, Van Roy N, De Paepe A, Speleman F. 2002. Accurate normalization of real-time quantitative RT-PCR data by geometric averaging of multiple internal control genes. *Genome Biology* **18**: 7.
- Vissenberg K, Martinez-Vilchez IM, Verbelen JP, Miller JG, Fry SC. 2000. *In vivo* colocalization of xyloglucan endotransglycosylase activity and its donor substrate in the elongation zone of *Arabidopsis* roots. *Plant Cell* **12**: 1229–1237.
- Yan D, Duermeyer L, Leoveanu C, Nambara E. 2014. The functions of the endosperm during seed germination. *Plant & Cell Physiology* **55**: 1521–1533.
- Yeung EC, Chan CKW. 2015. The glycol methacrylate embedding resins - Technovit 7100 and 8100. In: Yeung ECT, Stasolia C, Sumner MJ, Huang BQ, eds. *Plant microtechniques and protocols*. Heidelberg, Germany: Springer International, 67–82.
- Zhang Y, Chen B, Xu Z, Shi Z, Chen S, Huang X, Chen J, Wang X. 2014. Involvement of reactive oxygen species in endosperm cap weakening and embryo elongation growth during lettuce seed germination. *Journal of Experimental Botany* **65**: 3189–3200.

Supporting Information

Additional Supporting Information may be found online in the Supporting Information section at the end of the article.

Fig. S1 After-ripening and hormonal control of *Avena fatua* diaspore germination.

Fig. S2 Water uptake and organ expansion in D and AR coleorhizas and radicles.

Fig. S3 Flow cytometric analysis of DNA contents in leaf and coleorhiza.

Fig. S4 Images of ablated coleorhizas in *Avena fatua* caryopses.

Fig. S5 Example force-displacement curves of *Avena fatua* coleorhizas puncture force analysis.

Fig. S6 Transcript expression pattern of barley cell wall remodeling genes.

Fig. S7 Optimisation of the XET activity assay and xyloglucan oligosaccharide used.

Fig. S8 The effect of the xyloglucan oligosaccharides (XGO) on *Avena fatua* germination.

Table S1 Statistical analysis of stress applied to D and AR coleorhizas during biomechanical measurements.

Table S2 Primer sequences used for cloning and RT-qPCR.

Please note: Wiley Blackwell are not responsible for the content or functionality of any Supporting Information supplied by the authors. Any queries (other than missing material) should be directed to the *New Phytologist* Central Office.